Luminescent Chiral Ionic Ir(III) Complexes:

Synthesis and Photophysical Properties

Loredana Ricciardi,*[a] Massimo La Deda,[b] Andreea Ionescu,[b] Nicolas Godbert,[b] Iolinda Aiello,[b] Mauro Ghedini [b]

[a] *CNR NANOTEC-Istituto di Nanotecnologia U.O.S. Cosenza, 87036 Arcavacata di Rende (CS), Italy*
[b] *MAT-INLAB (Laboratorio di Materiali Molecolari Inorganici), LASCAMM and CR INSTM, Unità INSTM della Calabria, Dipartimento di Chimica e Tecnologie Chimiche, Università della Calabria, 87036 Arcavacata di Rende (CS), Italy*

Marco Fusè,*[c] Isabella Rimoldi,[c] Edoardo Cesarotti [c]

[c] *Dipartimento di Scienze Farmaceutiche, Università di Milano, Via Golgi 19, 20133 Milano, Italy*

Corresponding author at: CNR NANOTEC-Istituto di Nanotecnologia U.O.S. Cosenza, 87036 Arcavacata di Rende (CS), Italy (L.R.); Dipartimento di Scienze Farmaceutiche, Università di Milano, Via Golgi 19, 20133 Milano, Italy (M.F.).

Fax: +39 984 492066; Tel: +39 984 492897

E-mail address: loredana.ricciardi@unical.it; marco.fuse@unimi.it

Abstract

Three homologous series of luminescent octahedral ionic Ir(III) complexes (**1-12**) with a dual stereogenic center of general formula $^{\Delta,\Lambda\ (R,S)}$[(ppy)$_2$Ir(R-campy)]X, where ppy= 2-phenylpyridine, R-campy= 2-methyl-5,6,7,8-tetrahydroquinolin-8-amine (Me-campy) or 8-amino-5,6,7,8-tetrahydroquinolines (H-campy) and as counterions X^-= Cl$^-$ or CH$_3$COO$^-$ have been synthesized and characterized. The NMR characterization of each complex highlighted the diastereoisomeric purity and the absolute configuration has been confirmed by electronic circular dichroism spectroscopy. The absorption and the luminescence properties of the compounds in solution and in solid state have been investigated by UV-Vis, steady-state emission and time-correlated single-photon

counting spectroscopy. The obtained results from the twelve compounds highlight the difficult to correlate photophysical properties in solution to the stereochemistry, while excited states decay studies of the solid state samples indicate a correlation between photophysics and packing mode which is affected by the different stereochemistry.

1. Introduction

The outstanding photophysical properties of six-coordinated Ir(III) complexes have been widely highlighted within several fields of applications, including photoenergy conversion, advanced photonics and photocatalysis [1]. Moreover, in the last decades, extensive studies have demonstrated that the unique properties of this class of compounds, particularly with regard to their luminescence behaviour, render them appealing platforms for the development of labelling, sensing and bioimaging devices [2]. For these purposes, a great attention has been paid to the synthesis of complexes showing high solubilities in aqueous media, a requisite for such bio-related applications that can be achieved through an appropriate functionalization of the cyclometallated and ancillary ligands and/or induced by introducing into the molecular structures of the complexes a specifically chosen counterion [3,4].

Furthermore, with reference to the organometallic chemistry, an increasing interest recently raised towards the synthesis and characterization of chiral octahedral transition metal complexes. This research interest is fueled by the great potential of these optically active compounds to be used as asymmetric catalysts for enantioselective organic synthesis or to be employed in biomacromolecules selective recognition [5].

In this context, for example, structurally sophisticated Ru(II) or Ir(III) compounds as selective inhibitors of protein kinases have been reported [6] and a recent study has highlighted the use of enantiomers of octahedral Ir(III) complex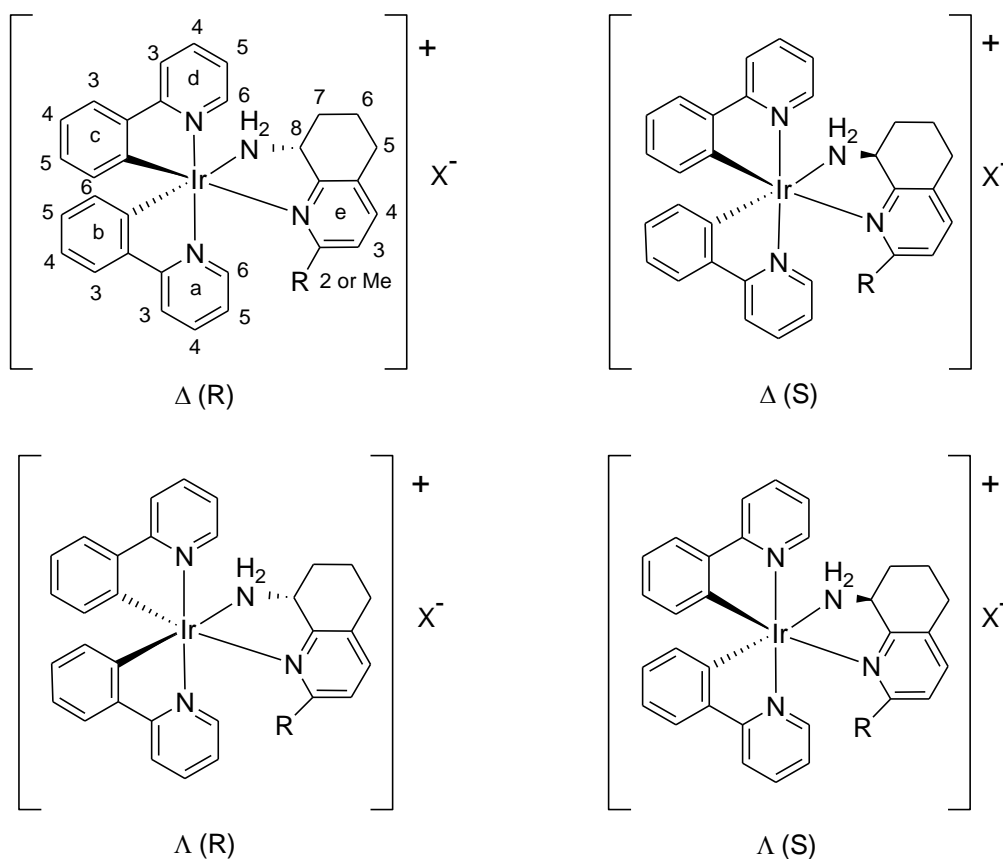es for the chiral discrimination of enzyme active sites [7]. Noteworthy, great efforts have been recently directed towards the exploration of other

organometallic architectures comprising a dual chiral information, the first chirality hold by the ligand, the second based onto the geometry of the metal centre, expanding in this manner the stereochemical complexity of the system but with the ultimate goal of obtaining highly selective chiral chemical probes [8].

Worthy of note that the presence in the same structure of two or more stereogenic centers combined with an efficient separation method, which affording to enantiomerically and diasteromerically pure species, provides the tremendous advantage of obtaining many isomers of one molecule possibly featuring different properties.

In this light, we report the synthesis and characterization of twelve new diastereopure chiral-at-metal complexes (**1**-**12**) (*Chart 1*), with the metal coordination sphere embedded by a chiral N,N ligand, giving rise to octahedral ionic Ir(III) complexes with a dual stereogenic center of general formula $^{\Delta,\Lambda\ (R,S)}$[(ppy)$_2$Ir(R-campy)]X, where ppy= 2-phenylpyridine, R-campy= 2-methyl-5,6,7,8-tetrahydroquinolin-8-amine (Me-campy) or 8-amino-5,6,7,8-tetrahydroquinolines (H-campy), and as counterions X$^-$= Cl$^-$ or CH$_3$COO$^-$. The complexes in their enantiomeric and diasteromeric forms were obtained in good yields and all the different stereoisomers were characterized by NMR and Electronic Circular Dichroism (ECD). Finally, the absorption and the luminescence properties of the compounds in solution and in solid state have been investigated by UV-Vis, steady-state emission and time-correlated single-photon counting spectroscopy, and interesting results about the role of the stereogenic centers have been obtained.

X⁻ = Cl⁻, R= CH₃: **1**= Δ-(R), **2**= Δ-(S), **3**= Λ-(R), **4**= Λ-(S);

X⁻ = Cl⁻, R= H: **5**= Δ-(R), **6**= Δ-(S), **7**= Λ-(R), **8**= Λ-(S);

X⁻ = CH₃COO⁻, R= H: **9**= Δ-(R), **10**= Δ-(S), **11**= Λ-(R), **12**= Λ-(S).

Chart 1. Chemical structures and proton numeration for the diasteroisomeric chiral Ir(III) complexes **1**-**12**.

2.   Experimental

Material and methods

Ir(III) chloride hydrate (IrCl₃·xH₂O) was purchased from Alfa Aesar. Unless otherwise stated, reagents and all the solvents were purchased from commercial sources and used without further purification. Enantiomerically pure 8-amino-5,6,7,8-tetrahydroquinolines (H-campy) and 2-methyl-5,6,7,8-tetrahydroquinolin-8-amine (Me-campy) were obtained as reported in the literature [9,10]. All synthesis involving Ir(III) complexes were carried out under nitrogen atmosphere using standard Schlenk techniques. [(ppy)₂Ir(μ-Cl)]₂ precursor was prepared according to the literature procedures

1 [11,12]. ^1H and ^{13}C-$\{^1H\}$ NMR spectra were recorded in $CDCl_3$, CD_3OD or a mixture of them on

2 Bruker DRX Advance 300 MHz equipped with a non-reverse probe or Bruker DRX Avance 400

3 MHz. Chemical shifts (in ppm) were referenced to residual solvent proton/carbon peak. Fast Atom

4 Bombardment Spectra (FAB) were acquired on a VG Autospec M246 spectrometer using p-

5 nitrobenzyl alcohol as the matrix. Elemental analyses (EA) were performed on Perkin Elmer Series

6 II CHNS/O Analyzer 2400 and ECD spectra in CH_2Cl_2 solution (10^{-4}M) were recorded at room

7 temperature on a Jasco J500 Spectrophotometer.

8

9 **Synthesis of diastereoisomeric mixture**

10 To a solution of $[(ppy)_2Ir(\mu\text{-}Cl)]_2$ (100 mg, 0.093 mmol) in CH_2Cl_2/MeOH (20 mL, 3:1 v/v) was

11 added an enatiomerically pure diamine, Me-campy or H-campy, (1.1 eq) and heated to reflux for 6

12 h [13]. The solution was allowed to cool to room temperature and the solvent evaporated. The

13 yellow residue was dissolved in 10 mL of CH_2Cl_2 and filtered. Solvent was partially evaporated up

14 to 2 mL then 5 mL of diethyl ether were added to obtain the products as yellow powder (yield up to

15 90%).

16 *NMR measurement of **2**,**4** mixture*

17 ^1H-NMR (400 MHz, $CDCl_3$) δ: 10.02 (d, J = 5.7 Hz, 1H), 9.90 (d, J = 5.6 Hz, 1H), 8.04 (d, J = 5.8

18 Hz, 1H), 7.97 (d, J = 8.2 Hz, 2H), 7.94 – 7.75 (m, 6H), 7.62 (d, J = 7.6 Hz, 1H), 7.58 – 7.52 (m,

19 3H), 7.50 – 7.41 (m, 3H), 7.39 (t, J = 6.2 Hz, 1H), 7.27 – 7.23 (m, 1H), 7.14 (t, J = 6.5 Hz, 1H),

20 7.05 – 6.99 (m, 2H), 6.96 – 6.83 (m, 6H), 6.81 – 6.60 (m, 5H), 6.26 (d, J = 7.8 Hz, 1H), 6.13 (d, J =

21 7.4 Hz, 2H), 6.01 (d, J = 7.8 Hz, 1H), 4.94 (m, 1H), 3.79 (s, 1H), 3.33 – 3.18 (m, 2H), 3.18 – 2.62

22 (m, 4H), 2.27 – 2.16 (m, 1H), 2.16 – 1.90 (m, 4H), 1.87 (s, 3H), 1.71 (s, 3H), 1.70 – 1.51 (m, 5H).

23 MS (FAB): m/z 663 $[M]^+$, 501 $[Ir(ppy)_2]^+$. CHN calculated: C 54.82%, H 4.33%, N 7.97% found: C

24 55.04%, H 4.33%, N 8.02%. Identical results have been obtained for **1**,**3** disteromeric mixture.

25 *NMR measurement of **6**,**8** mixture*

^{1}H-NMR (400 MHz, CDCl$_3$) δ: 10.37 – 9.94 (m, 2H), 8.02 (d, J = 7.8 Hz, 1H), 7.97 – 7.84 (m, 4H), 7.84 – 7.71 (m, 4H), 7.68 (d, J = 7.7 Hz, 1H), 7.66 – 7.60 (m, 2H), 7.60 – 7.54 (m, 2H), 7.51 (d, J = 7.6 Hz, 2H), 7.44 (d, J = 4.9 Hz, 1H), 7.40 – 7.33 (m, 1H), 7.15 – 7.07 (m, 3H), 7.07 – 6.94 (m, 5H), 6.94 – 6.83 (m, 3H), 6.83 – 6.68 (m, 5H), 6.48 (d, J = 7.4 Hz, 1H), 6.30 (d, J = 7.5 Hz, 1H), 6.19 (d, J = 7.6 Hz, 2H), 4.74 (s, 1H), 3.93 (s, 1H), 3.48 – 3.38 (m, 1H), 3.38 – 3.23 (m, 1H), 3.08 – 2.90 (m, 2H), 2.90 – 2.67 (m, 4H), 2.12 – 1.99 (m, 2H), 1.97 – 1.78 (m, 2H), 1.73 – 1.62 (m, 2H). MS (FAB): m/z 649 [M]$^+$, 501 [Ir(ppy)$_2$]$^+$. CHN calculated: C 54.41%, H 4.12%, N 8.19% found: C 54.1%, H 4.12%, N 8.12%. Identical results have been obtained for **5,7** disteromeric mixture.

General procedure for diastereomers separation with potassium (+)-10-camphorsulfonate

In a solution of $^{\Delta,\Lambda}$[(ppy)$_2$Ir(R-campy)]Cl (50mg) in CH$_2$Cl$_2$/MeOH (10 mL, 3:1 v/v) were added 3 eq of potassium (+)-10-camphorsulfonate and heated to reflux for 1 h. The solution was allowed to cool to room temperature and the solvent evaporated. The light yellow residue was suspended in 10 mL of acetone. The yellow precipitate constituted by the first camphorsulfonate diastereomer was filtered off and washed three times with acetone. The resulting acetone solutions were combined, solvent was evaporated and the thus obtained yellow residue was redissolved in 3 mL of acetone and filtered. Once the solvent evaporated, the second counterpart camphorsulfonate diastereomer was obtained. Finally, both camphorsulfonate salts were stirred in a biphasic mixture of H$_2$O/CH$_2$Cl$_2$ (20 mL,1:1 v/v) with 10 eq. of NH$_4$Cl. The organic phase was dried over anhydrous Na$_2$SO$_4$, the solvent was partially evaporated up to 1 mL and 5 mL of diethyl ether were added to obtain the corresponding chloride product as yellow powder. The diastereomeric ratios were determined by ^{1}H-NMR spectroscopy in CDCl$_3$/CD$_3$OD (3:1 v/v).

*NMR measurement of **2***

Obtained from the soluble camphorsulfonate derivative. Yellow solid, yield 22 mg (44%). ^{1}H-NMR (300 MHz, CDCl$_3$) δ: 9.91 (d, J = 6.4 Hz, 1H, a6), 8.03 (d, J = 5.8 Hz, 1H, d6), 7.99 – 7.75 (m, 4H, d3/a3/d4/a4), 7.60 (d, J = 7.1 Hz, 1H, b3), 7.53 (d, J = 6.8 Hz, 1H, c3), 7.45 (d, J = 7.8 Hz, 1H, e4),

7.38 (t, J = 5.9 Hz, 1H, a5), 7.14 (t, J = 6.6 Hz, 1H, d5), 6.92 (d, J = 7.9 Hz, 1H, e3), 6.84 (t, J = 7.5 Hz, 2H, b4/c4), 6.70 (m, 2H, b5/c5), 6.49 (t, J = 12.1 Hz, 1H, NH), 6.11 (d, J = 7.7 Hz, 1H, b6), 6.00 (d, J = 7.8 Hz, 1H, c6), 3.77 (m, 1H, e8), 3.22 (d, J = 12.1 Hz, NH), 3.02 (m, 2H, e5/e7), 2.72 (d, J = 16.7 Hz, H, e5'), 2.17 – 2.10 (m, 1H, e7'), 1.99 (m, 1H, e6), 1.71 (s, 3H, Me), 1.58 (m, 1H, e6'). ^{13}C-NMR (75 MHz, CDCl$_3$) δ: 169.22, 168.23, 160.99, 160.20, 154.33, 153.76, 149.51, 144.71, 144.49, 143.10, 139.71, 138.19, 137.81, 134.31, 132.62, 131.04, 130.82, 129.95, 125.48, 124.93, 124.57, 123.63, 123.27, 122.61, 121.26, 120.33, 118.84, 58.69, 32.78, 28.82, 26.52, 22.18. CHN calculated: C 55.04%, H 4.33%, N 8.02% found: C 54.8%, H 4.33%, N 7.98%. Identical results have been obtained for **3**.

NMR measurement of 4

Obtained from the precipitated camphorsulfonate derivative. Yellow solid, yield 23 mg (46%). ^{1}H NMR (300 MHz, CDCl$_3$/CD$_3$OD, 3:1 v/v) δ 9.26 (d, J = 5.2 Hz, 1H, a6) [in CDCl$_3$ at 9.77 ppm], 7.93 (d, J = 8.1 Hz, 1H, d3), 7.88 – 7.71 (m, 3H, a3/d4/a4), 7.58 – 7.47 (m, 2H, c3/b3), 7.46 – 7.35 (m, 2H, d6/a5), 7.26 (m, 1H, e4), 7.07 – 6.94 (m, 2H, d4/e2), 6.81 (d, J = 2.8 Hz, 2H, b4/c4), 6.67 (dd, J = 7.9, 7.4 Hz, 2H, b5/c5), 6.11 (d, J = 7.8 Hz, 1H, b6), 6.07 (d, J = 7.4 Hz, 1H, d6), 5.98 (s, 1H, NH), 4.75 (s, 1H, e8), 3.05(m, 1H, NH), 2.77 (s, 2H, e7/e5), 2.68 (m, 1H, e5), 1.93 (s, 2H, e5/e6), 1.82 (s, 3H, Me) [in CDCl$_3$ at 1.87 ppm], 1.59 (s, 1H, e5). ^{13}C-NMR (75 MHz, CDCl$_3$) δ 169.30, 169.24, 161.72, 160.31, 155.27, 153.03, 148.18, 144.06, 143.98, 143.05, 139.69, 138.22, 137.93, 133.69, 132.44, 131.75, 130.58, 130.13, 126.23, 124.61, 124.41, 123.64, 123.11, 122.38, 121.51, 120.11, 119.25, 58.66, 33.67, 28.45, 28.21, 21.64. CHN calculated: C 55.04%, H 4.33%, N 8.02% found: C 54.92%, H 4.33%, N 8.00%. Identical results have been obtained for **1**.

NMR measurement of 6

Obtained from soluble camphorsulfonate derivative. Yellow solid, yield 22 mg (44%). ^{1}H-NMR (300 MHz, CDCl$_3$) δ: 10.08 (d, J = 4.8Hz, 1H, a6), 7.99 (d, J = 8.0 Hz, 1H, d3), 7.88 (m, 3H, a3/d6/d4), 7.78 (t, J = 7.5 Hz, 1H, a4), 7.69 (d, J = 7.6 Hz, 1H, b3), 7.62 (d, J = 7.7 Hz, 1H, c3), 7.51 (d, J = 7.6 Hz, 1H, e4), 7.45 (d, J = 5.1 Hz, 1H, e2), 7.39 (m, 1H, a5), 7.10 (t, J = 6.2 Hz, 1H,

d5), 7.03 – 6.93 (m, 2H, e3/b4), 6.89 (t, J = 7.2 Hz, 1H, c4), 6.78 (t+m, J = 7.4 Hz, 3H, b5/c5/NH),

6.31 (d, J = 7.5 Hz, 1H, c6), 6.18 (d, J = 7.5 Hz, 1H, b6), 3.92 (m, 1H, e8), 3.30 (m, 1H, NH), 3.00

(m, 2H, e7/e5), 2.75 (m, 1H, e5'), 2.30 (m, 1H, e7'), 2.06 (m, 1H, e6), 1.64 (m,1H, e6'). ^{13}C-NMR

(75 MHz, CDCl$_3$) d 170.12, 167.20, 160.54, 154.04, 151.97, 148.97, 148.32, 147.23, 144.57, 143.57,

138.43, 138.21, 137.79, 137.68, 133.92, 131.78, 130.80, 129.98, 124.96, 124.73, 124.12, 122.72,

122.35, 122.09, 120.13, 119.03, 58.38, 31.84, 28.42, 22.55. CHN calculated: C 54.41%, H 4.12%,

N 8.19% found: C 53.96%, H 4.22%, N 8.07%. Identical results have been obtained for **7**.

NMR measurement of 8

Obtained from the precipitated camphorsulfonate derivative. Yellow solid, yield 23 mg (46%). ^{1}H-

NMR (300 MHz, CDCl$_3$) δ: 10.13 (d, J = 5.5 Hz, 1H, a6) [in CDCl$_3$/CD$_3$OD 3:1 9.16 ppm], 7.92 (d,

J = 8.3 Hz, 1H, d3), 7.78 (m, 3H, a3/d4/a4), 7.58 (m, 3H,c3/b3/e2), 7.46 (m, 2H, a5/e4), 7.09 (m,

2H, e3/d6), 7.04 – 6.90 (m, d5/c4/NH) [NH in CDCl$_3$/CD$_3$OD 3:1 5.82 ppm], 6.90 – 6.74 (m, 3H,

b4/b5/c5), 6.51 (d, J = 6.7 Hz, 1H, c6), 6.18 (d, J = 7.2 Hz, 1H, b6), 4.65 (m, 1H, e8), 3.50 (m, 1H,

NH), 2.77 (m, 3H, e5/e5'/e7), 2.04 – 1.6 (m, 3H, e7', e6, e6'). ^{13}C-NMR (75 MHz, CDCl$_3$) δ 168.49,

162.52, 154.96, 153.66, 148.20, 148.04, 147.53, 144.81, 143.57, 138.12, 138.00, 137.57, 136.90,

133.03, 132.04, 130.60, 130.52, 125.20, 124.45, 124.45, 124.32, 122.71, 122.01, 121.94, 119.86,

118.99, 58.96, 32.51, 28.26, 22.47. CHN calculated: C 54.41%, H 4.12%, N 8.19% found: C 54.7%,

H 4.18%, N 8.22%. Identical results have been obtained for **5**.

Synthesis of 9-12 diastereoisomeric mixture

In a solution of optically pure [(ppy)$_2$Ir(H-campy)]Cl (25 mg, 3.7 E-2 mmol) in methanol (5mL) 1.1

eq of silver acetate were added, the reaction mixture, protected from light, was further stirred for 2

hours. Then the solvent was evaporated, CH$_2$Cl$_2$ was added and the AgCl formed was filtered out.

The pure products were obtained by subsequent recrystallizations from CH$_2$Cl$_2$/n-Hexane.

NMR measurement of 10

^{1}H-NMR (300 MHz, CDCl$_3$) δ: 10.03 (d, J = 5.4 Hz, 1H, a6), 7.99 (d, J = 6.7 Hz, 1H, d3), 7.94 – 7.75 (m, 5H, a3/d6/d4/a4/NH), 7.71 – 7.57 (m, 2H, b3/c3), 7.51 (d, J = 4.0 Hz, 1H, e4), 7.47 – 7.34 (m, 2H, e2/a5), 7.16 – 7.04 (m, 1H d5), 7.04 – 6.83 (m, 3H, e3/b4/c4), 6.83 – 6.72 (m, 2H, b5/c5), 6.29 (d, J = 6.6 Hz, 1H, c6), 6.16 (d, J = 7.6 Hz, 1H, b6), 3.99 – 3.81 (m, 1H, e8), 3.10 – 2.88 (m, 3H, NH/e7/e5), 2.84 – 2.61 (m, 1H, e5'), 2.30 (m, 1H, e7'), 2.08 (s, 3H, CH$_3$COO), 2.07 (s, 1H, e6), 1.66 (m, 1H, e6'). CHN calculated: C 55.99%, H 4.41%, N 7.91% found: C 55.88%, H 4.41%, N 7.89%. Identical results have been obtained for **11**.

NMR measurement of 12

^{1}H-NMR (400 MHz, CDCl$_3$) δ: 9.80 (d, J = 5.4 Hz, 1H, a6), 7.94 (d, J = 8.2 Hz, 1H, d3), 7.81 (t, J = 8.5 Hz, 1H, a3), 7.76 (dd, J = 14.5, 7.3 Hz, 2H, d4/a4), 7.71 – 7.55 (m, 5H, NH/e2/d4/b3/c3), 7.51 (d, J = 7.9 Hz, 1H, e4), 7.44 (t, J = 6.0 Hz, 1H, a5), 7.17 – 7.07 (m, 2H, e3/d6), 7.03 – 6.92 (m, 2H,d5/c4), 6.92 – 6.76 (m, 3H,c5/b5/b4), 6.47 (d, J = 7.2 Hz, 1H, c6), 6.23 (d, J = 7.7 Hz, 1H, b6), 4.79 (s, 1H, e8), 3.04 (t, J = 12.0 Hz, 1H, NH), 2.96 – 2.67 (m, 3H, e5/e5'/e7), 2.08 – 1.90 (m, 3H, CH$_3$COO$^-$), 1.83 (s, 2H, e7', e6), 1.74 – 1.53 (m, 1H, e6'); CHN calculated: C 55.99%, H 4.41%, N 7.91% found: C 55.87%, H 4.42%, N 7.89%. Identical results have been obtained for **9**.

Photophysical studies

Spectrofluorimetric grade solvents were used for the photophysical investigations in solution, at room temperature. A Perkin Elmer Lambda 900 spectrophotometer was used to obtain the absorption spectra. Steady-state emission spectra were recorded on a HORIBA Jobin-Yvon Fluorolog-3 FL3-211 spectrometer equipped with a 450 W xenon arc lamp, double-grating excitation and single-grating emission monochromators (2.1 nm/mm dispersion; 1200 grooves/mm), and a Hamamatsu R928 photomultiplier tube. Emission and excitation spectra were corrected for source intensity (lamp and grating) and emission spectral response (detector and grating) by standard correction curves. To prevent that second order diffraction light from the source could reach detector, cut/off filters were used, if necessary.

1 Emission quantum yields values (Φ) were determined using the optically dilute method [14];

2 Ru(bpy)$_3$Cl$_2$ in air-equilibrated water solution was used as standard (Φ = 0.028) [15].

3 Time-resolved measurements were performed using the time-correlated single-photon counting

4 (TCSPC) option on the Fluorolog 3. NanoLED at 379 nm, fwhm <200 ps with repetition rate at 1

5 MHz, was used to excite the sample. Excitation source was mounted directly on the sample

6 chamber at 90° to a single-grating emission monochromator (2.1 nm/mm dispersion; 1200

7 grooves/mm) and the emission was collected with a TBX-04-D single-photon-counting detector.

8 The photons collected at the detector were correlated by a time-to-amplitude converter (TAC) to the

9 excitation pulse. Signals were collected using an IBH Data Station Hub photon counting module,

10 and data analysis was performed using the commercially available DAS6 software (HORIBA Jobin

11 Yvon IBH). The quality of the fit was assessed by minimizing the reduced χ2 function and visual

12 inspection of the weighted residuals. With regard to the solid state measurements, the samples were

13 prepared by placing a given amount of powder between two quartz slides and standardizing the

14 layer.

15

16 ## 3.   Results and Discussion

17 **Synthesis**

18 The ionic Ir(III) complexes were synthesized starting from binuclear chloro-bridged Ir(III) complex

19 [Ir(ppy)$_2$(μ-Cl)]$_2$ according to the procedure used for the related 2-picolylamine complex [13]. The

20 bridge splitting reaction was conducted by using two molar equivalents of the diamine ligands in

21 their enantiomeric pure form: (*R*) or (*S*)-2-methyl-5,6,7,8-tetrahydroquinolin-8-amine (Me-campy)

22 to yield to complexes **1**-**4** and (*R*) or (*S*)-8-amino-5,6,7,8-tetrahydroquinolines (H-campy) [10] to

23 respectively yield to complexes **5**-**8**. The diastereomeric mixtures were characterized by ^{1}H-NMR,

24 FAB and EA. The starting chloro-bridged dinuclear Ir(III) complex is a racemic Δ/Λ mixture, thus

25 the reaction with a stoichiometric amount of a chiral ligand give rise to a 50:50 diastereomeric

mixture of complexes, as proven by the ^{1}H-NMR spectroscopy performed in deuterated $CDCl_3$. The ^{1}H-NMR spectra in $CDCl_3$ evidenced the different solubility of the diastereomeric couples, where an apparent percent diastereomeric excess (d.e.%) can be observed in saturated solution. However in the chloride complexes this solubility difference did not allow the complete separation, that was achieved by substituting the chloride ion by the corresponding camphorsulfonate counteranion via metathetical reaction. The diastereomers were thus separated by selective precipitation in acetone. Finally the chloride complexes were restored with a large excess of ammonium chloride. The acetate derivatives (**9**-**12**) were synthesized by metathetical reaction of the pure chloride diastereomer with silver acetate following the literature procedure [4]. All the diastereomers were fully characterized by NMR, FAB spectrometry and EA.

NMR characterization

Despite the number of signals due to the loss of symmetry, all the signals were assigned by COSY, NOESY, HSQC, HMBC analysis (see SI section 1). Compared to the starting dinuclear complex, all compounds (see Chart 1 for the proton numbering scheme) showed a considerable high frequencies chemical shift for the H^{a1} ($\approx$10 ppm) and for one H^{NH} proton (7 ppm) and the characteristic shielding of the proton next to the metal in the ortometallated phenyl-ring [16]. In the chloride diastereomers **1**-**8** the chemical shifts are strongly affected by the polarity of the deuterated solvent. When to $CDCl_3$ was added to CD_3OD (in the ratio 3:1 v/v) both protons H^{a1} and H^{NH} moved to lower frequencies of 0.97 and 1.08 ppm respectively, and the same behaviour was observed for all the remaining complexes. The switch to a more polar solvent increases the ion solvation, thus the high frequencies shift could be attributed to a strong interaction with the counter anion, which was confirmed by Density Functional Theory (DFT) calculation (see SI section 2). The signals of the asymmetric proton in the diamine ligand H^{e8} showed the greater differences in the diastereomer NMR spectra, showing a chemical shift of *ca.* 0.9 ppm in **1**-**4** and 0.7 ppm in the case of **5**-**8**.

The differences could be due to a greater influence exerted by the ring current of a neighbour pyridine ring on one of the diastereomers or to a different interaction with the chloride ion; however

the small changes in the chemical shift in the (+)-10-camphorsulfonate or acetate complexes seem

to corroborate the first hypothesis. With an (*S*) amine configuration, an attribution to the Δ−complex

of the low frequency shifted signal could be guessed observing the relative position of H^{e8} and

pyridine ring in a molecular model.

All complexes showed a specific pattern of NOE cross-peaks, in which the presence or the lack of

cross-peak between H^{a1} and H^{e8} was particularly useful for an unambiguous identification. The

chiral ancillary ligand interacts in different ways with the chiral $[Ir(ppy)_2]^+$ moiety depending on its

chirality; with (*S*) H-campy or (*S*) Me-campy a NOE between H^{a1} and H^{e8} can be observed only if

the Ir(III) center has an Λ configuration; an opposite metal configuration would bear these two

protons too far away from eachother to give rise to a NOE effect (see SI section 1). Thus if the

diamine configuration is (*S*) the presence of cross-peak state the metal configuration as Λ, otherwise

the configuration of the metal centre must be Δ. Furthermore, the H^{e8} chemical shifts were found as

up frequencies and low frequencies shifted in Λ and Δ configurations respectively, as previously

predicted by the DFT calculations.

Electronic Circular Dichroism spectroscopy (ECD)

The ECD proved the opposite configuration of the metal center in the couple of diastereomers.

The coherence of the NMR based configuration assignment was proved by the perfect mirror image

shape of two complexes identified as enantiomers by NMR such as the couples **1**/**4** and **6**/**7**.

Moreover, it was possible to observe a preponderance of the metal ellipticity role over the ancillary

ligand contribution. Three regions of the spectrum could be recognised: below 300 nm, around 350

nm and over 400 nm in which the sign of the ECD inverts. If the metal chirality was kept constant

(**1**/**2**) the sign of the ECD spectra remained the same in all the regions, on the contrary if the

diamine configuration was kept constant the ECD signs inverted. This was also true changing from

Me-campy to H-campy ligand; **7** and **8** showed similar ECD profile. With the aim to isolate the

different contribution, the spectrum of the crude diasteromeric mixture product $^{\Delta,\Lambda\,(S)}[(ppy)_2Ir(H-

campy)]Cl was recorded. Due to the racemic metal center the ECD spectrum represented mainly the contribution of the optically pure diamine ligand. The spectra are showed in Figures 1-3. The ancillary ligand influences the overall ECD response [17], however, mainly in the regions below 300 nm and over 380 nm, where the intensity ratio is indeed higher (Fig. 2). Consequently the sign of the ECD spectrum at 350 nm could be taken as descriptor of the chirality at the metal center. According to related bis-cyclometalated Ir(III) complexes, for which the crystallographic structures are known [17,18], the sequence of signs + (< 300 nm), - (350 nm), + (> 400 nm) can be related to a Δ configuration. These data are consistent with the configuration assigned by the NMR analysis and allow to unequivocally assign the absolute metal configuration. The counter anion change did not affect significantly the ECD spectrum (Fig.3).
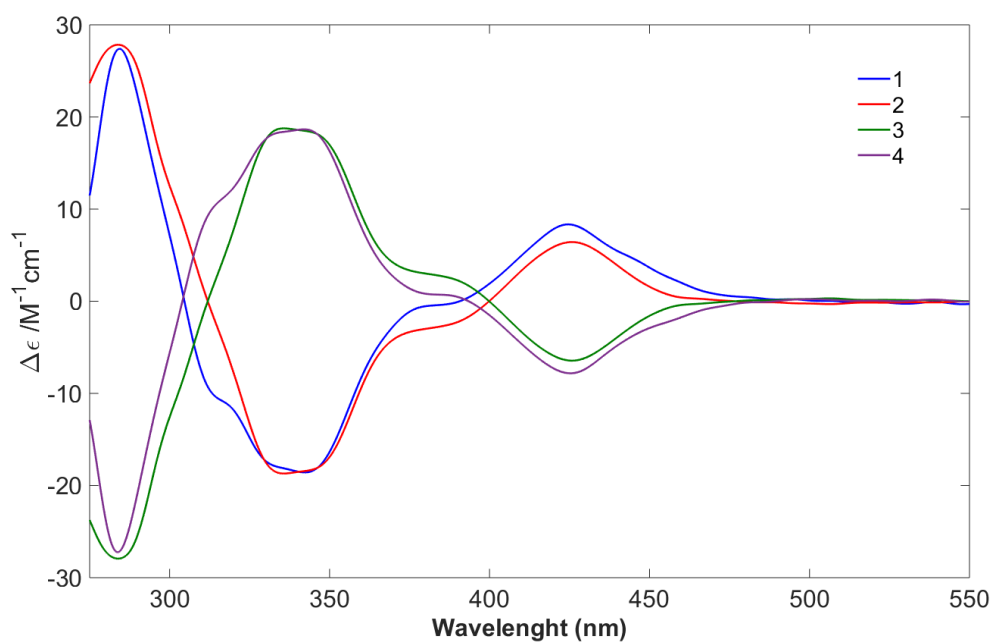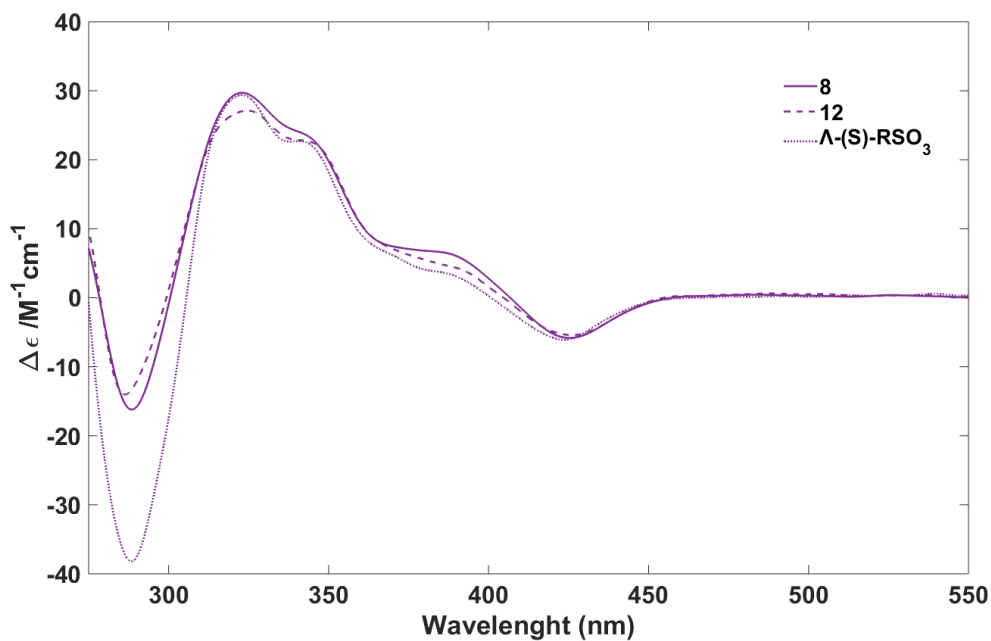

Figure 1. ECD spectra of complexes **1**-**4**.
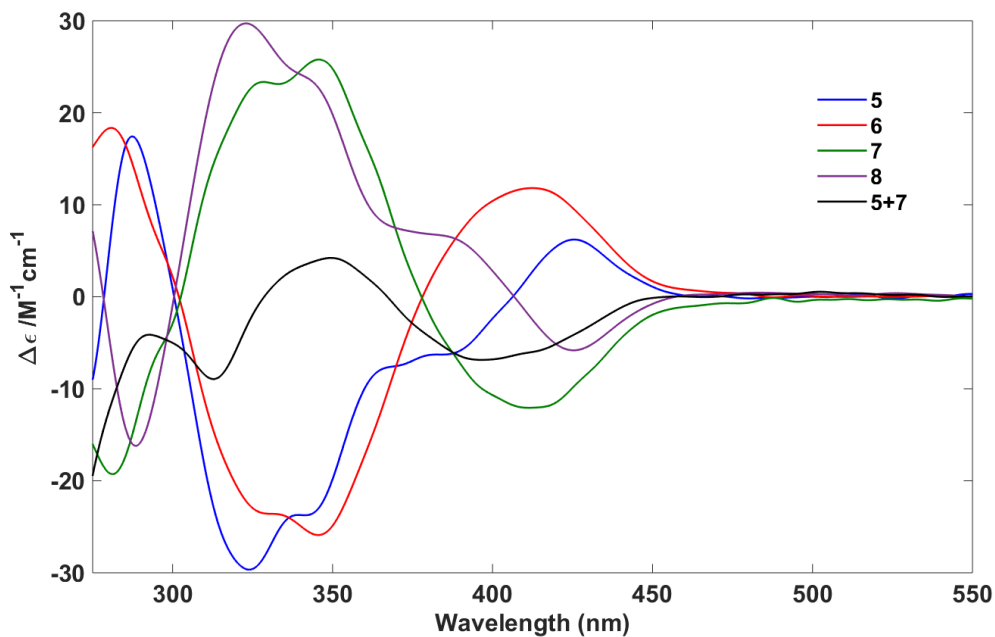
Figure 2. ECD spectra of complexes **5**-**8** and **5**+**7**.

Figure 3. ECD spectra of complexes **8,12** and $^{\Lambda\ (S)}$[(ppy)$_2$Ir(H-campy)] (+)-10-camphorsulfonate (Λ-(*S*)-RSO$_3$); the change of counter anion does not highly affected the band shape, (+)-10-camphorsulfonate transitions lie below 320 nm.

Photophysical characterization

1   All the considered compounds (**1**-**12**) were dissolved in spectroscopic grade solvent, *i.e.*

2   dichloromethane for the chloride complexes (**1**-**8**) or water for the acetate ones (**9**-**12**), and

3   absorption bands are reported in Table 1.

4

5   **Table 1**. Photophysical data in air-equilibrated solution at room temperature

	Absorption: λ/nm(ε/M^{-1}cm^{-1})	Emission: λ/nm	τ/ns	Φ
1[a]	264(35160), 293(s), 312(s), 346(6109), 390(3424), 423(2585), 476(s)	495, 518	58.6	2.9 %
2[a]	264(34474), 293(s), 312(s), 346(5990), 390(3357), 423(2535), 476(s)	495, 518	52.5	2.7 %
3[a]	264(34627), 293(s), 312(s), 346(6016), 390(3372), 423(2546), 476(s)	495, 518	51.9	2.7 %
4[a]	264(33798), 293(s), 312(s), 346(5872), 390(3292), 423(2485), 476(s)	495, 518	60.6	3.1 %
5[a]	261(24413), 293(s), 312(s), 346(4378), 390(2751), 423(2086), 476(s)	495, 515	90.7	6.1 %
6[a]	261(24053), 293(s), 312(s), 346(4313), 390(2710), 423(2056), 476(s)	495, 515	94.4	6.3 %
7[a]	261(23767), 293(s), 312(s), 346(4262), 390(2678), 423(2031), 476(s)	495, 515	95.6	6.3 %
8[a]	261(23604), 293(s), 312(s), 346(4233), 390(2659), 423(2017), 476(s)	495, 515	89.2	6.0 %
9[b]	259(34254), 288(s), 306(s), 342(5778), 386(3933), 418(2879), 471(s)	490, 510	433	15.3 %
10[b]	259(33549), 288(s), 306(s), 342(5659), 386(3852), 418(2819), 471(s)	490, 510	435	15.4 %
11[b]	259(34556), 288(s), 306(s), 342(5829), 386(3968), 418(2904), 471(s)	490, 510	422	14.9 %
12[b]	259(34052), 288(s), 306(s), 342(5744), 386(3910), 418(2862), 471(s)	490, 510	413	14.7 %

6   [a]dichloromethane; [b]water; s:shoulder.

7

8   No relevant differences are detected among the studied complexes, except a slight shift of the

9   higher energy band which position depends on the ligand substituents, solvent and counterion, but

10   no on the isomerism. In Figure 4 are reported the absorption profiles of complexes **2**, **6** and **10**,

11   representative of each of the three series according to the substituents and the counterion: the sharp

12   and intense band at 264 (or 261 or 259) nm (with a series of shoulders below 350 nm) is attributed

13   to spin-allowed π,π^* transitions of the ppy ligands [19].
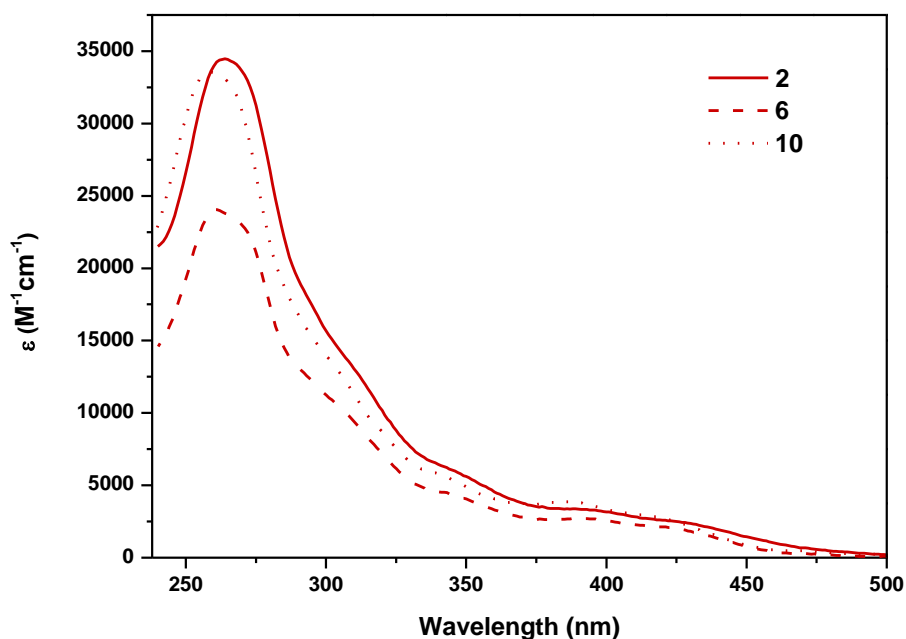
Figure 4. Absorption spectra of the complexes **2**, **6** in dichloromethane and **10** in water solution at room temperature.

At higher wavelengths (from 350 to 500 nm), weaker bands are observed. The assignment of these bands is not straightforward, as reported by various authors [20], because their low intensity rules out spin-allowed π,π^* transitions, and on the other hand, pure MLCT transitions are unlikely because of their solvent insensitivity and their structured features: in our case, it seems reasonable to attribute to these bands a mixed (MLCT-LC) character [21]. Molar absorptivity which is almost identical for **1**-**8**, is reduced for **9**-**12**, probably depending on solvent.

It is known that cyclometalated octahedral Ir(III) complex in solution often display aggregation phenomena which strongly affect their photophysical properties [4]. Luminescence spectra have been recorded from 1.0 E-5 M solutions, and, in order to probe possible aggregation phenomena, results were compared with the emission from 1.0 E-6 M solutions. For all complexes except **1** and **4**, dilution does not modify spectral shape: the low concentrated solutions of **1**-**12** show two vibronic peaks emission, the first in the 490-495 nm range, and the second in the 510-518 nm range,

1 depending of the substituent and of the counterion (see Table 1), but the shape or the maxima

2 position of the spectra (Fig. 5) are not affected by the chirality of the isomers.
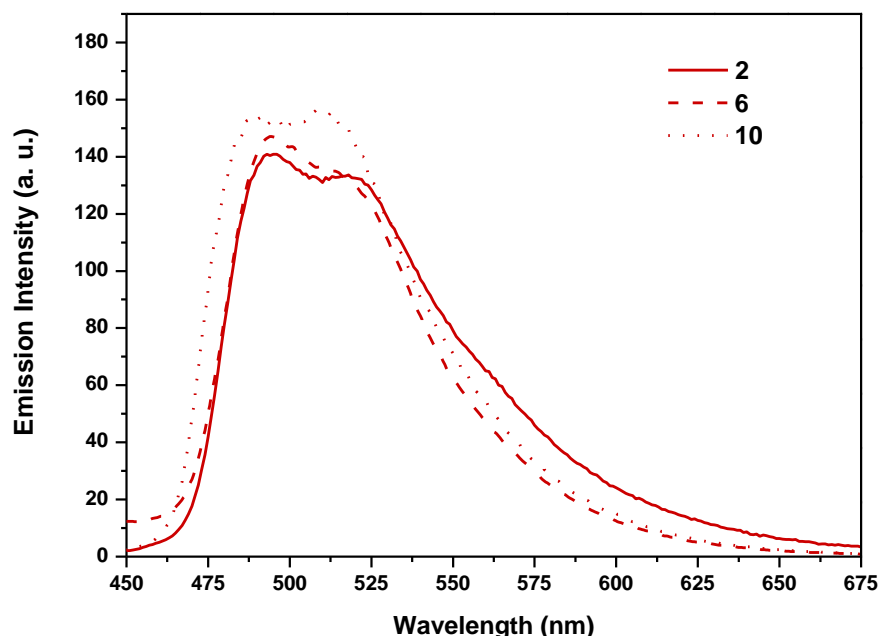

3

4 **Figure 5.** Emission spectra of the three isomers **2**, **6** in air-equilibrated dichloromethane and **10** in water

5 solution at room temperature.

6

7 Remarkably, 1.0 E-5 M solutions of **1** and **4,** show a unique peak at 515 nm (see SI section 5). This

8 behavior is attributed to a reduced solubility of this enantiomeric couple with respect to the other

9 enantiomeric couple with the same substituents and counterion (**2** and **3**), suggesting a role of the

10 chirality in the aggregation modes that affects photophysics (see below).

11 The luminescence profiles of the spectrum exhibit a vibronic resolution which is typical for Ir(III)-

12 ppy complexes [3,19,22], and taking into account the lifetime values from air-equilibrated solution

13 (Table 1), the emission is assigned to a mixed ^{3}(MLCT-LC) state. Lifetime values in air-

14 equilibrated solution can be grouped into three ranges, according to substituents or counterions, not

15 to chirality. In particular, complexes **1**-**4** show lifetime decays in the range 51.9-60.6 ns, complexes

16 **5**-**8** in the range 89.2-95.6 ns, and complexes **9**-**12** in the range 413-435 ns; analogously, emission

17 quantum yield (EQY) values follow the same trend, ranging from 2.7-3.1% in the first series, 6.0-

1 6.3% for the second one, 14.7-15.4 for the last one. As previously observed for similar compounds

2 [3], in contrast, acetate complexes in water solution show considerably higher lifetime and EQY

3 values. Once again, differences among complexes are due to different substituents or counterions,

4 not to chirality.

5 Since we observed that a different solubility of the complexes due to their stereoisomerism might be

6 reflected on a different emission spectrum shape in solution; to investigate possible effects of

7 chirality on the luminescence, a photophysical study on solid samples was performed.

8 Luminescence spectra of solid samples, reported in Figure 6-8 show a quite complicated vibronic

9 structure, probably due to the various packing mode involving chromophoric synthons that

10 consequently influenced differently the de-excitation of the mixed ^{3}(MLCT-LC) states.
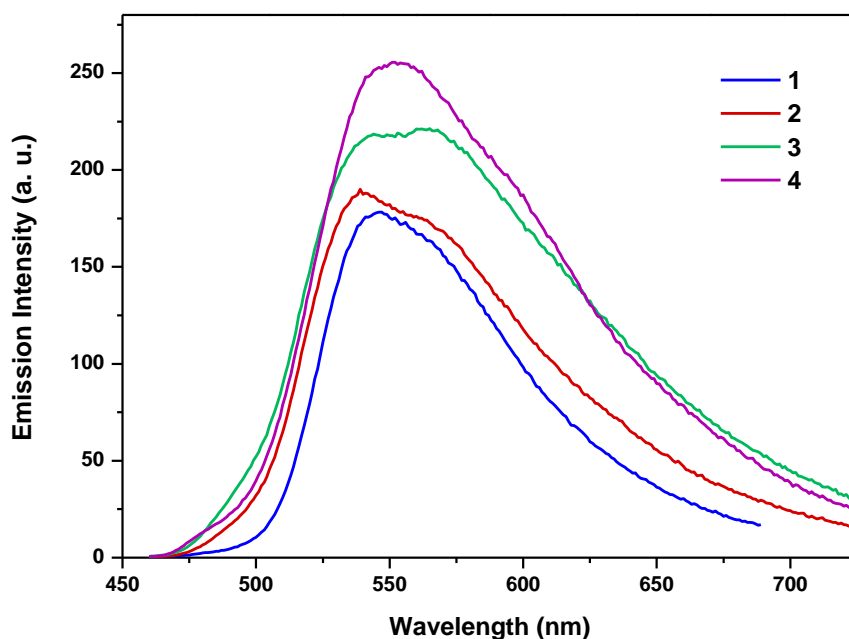
11

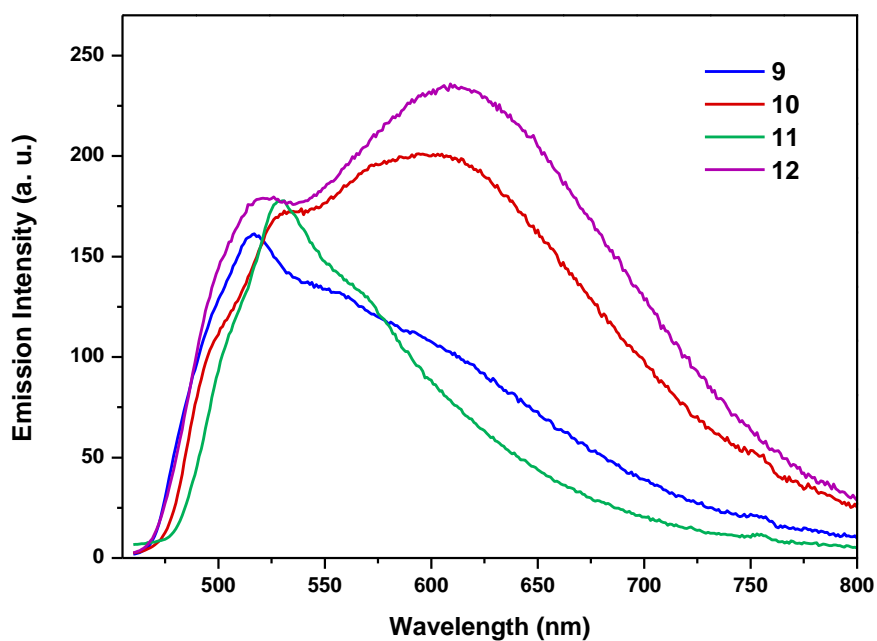12 **Figure 6.** Luminescence spectra of solid samples **1**-**4**.
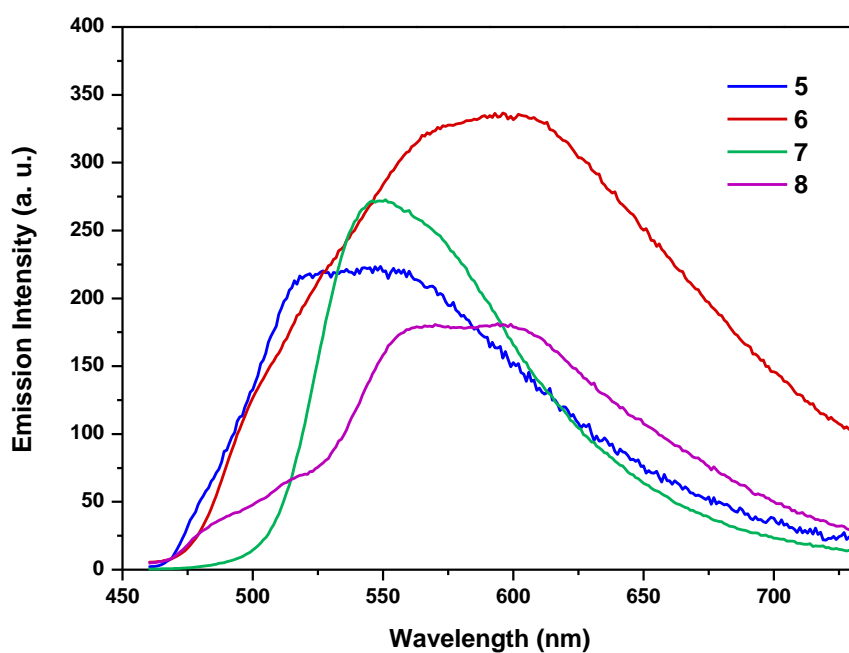
Figure 7. Luminescence spectra of solid samples **5**-**8**.

Figure 8. Luminescence spectra of solid samples **9**-**12**.

To better highlight the similarity among the spectra of the three series of compounds, four spectral

zones can been identified (the first zone, α, includes the 470-510 nm range; the second, β, includes

1   the 510-530 nm range; the third, γ, includes the 530-570 nm range; the fourth, δ, includes the 570-

2   620 nm range), in which of them is present a band of different intensity, depending on the

3   compound and on the stereoisomerism. The convolution of the bands observed in each zone

4   attributed with different intensities would produce spectra with a rather different shape. In Table 2

5   the band positions for **1**-**12** are compiled according to these 4 zones, illustrating that all compounds,

6   except **7**, have a spectral feature in each of the four zones, that appears either as a principal band

7   (p), as a shoulder (s) or as a weak signal (w) covered by another band.

8

9   **Table 2**. Emission bands in solid sample

	Spectral range*			
	α	β	γ	δ
1	490 (s)	w	546 (p)	563 (s)
2	493 (s)	w	540 (p)	563 (s)
3	494 (s)	w	543 (p)	565 (p)
4	484 (s)	w	554 (p)	600 (s)
5	486 (s)	w	524 (p)	553 (p)
6	504 (s)	533 (s)	574 (p)	603 (p)
7	-	-	548 (p)	570 (s)
8	490 (s)	515 (s)	568 (p)	597 (p)
9	498 (s)	516 (p)	554 (s)	603 (s)
10	500 (s)	533 (p)	570 (s)	598 (p)
11	508 (s)	530 (p)	560 (s)	w
12	500 (s)	521 (p)	w	610 (p)

10   *p:principal; s:shoulder; w:weak or undetectable

11

12   For each solid sample the emission lifetimes were measured in each defined spectral zone and the

13   recorded values are reported in Table S2 (see SI). Obtained results shown that emission lifetimes

14   are significantly different from one zone to another. Excited-state decays were invariably fitted by a

15   three-exponential function, and, in most cases, **10** showed the shorter lifetimes, while **11** the longer

16   ones. Since it is reasonable to assume that the four spectral regions refer to similar de-excitation

17   pathways, the estimation of the emission lifetime values in the α, β, γ and δ zones have been

18   performed. Table 3 collects lifetime obtained by averaging the values within every spectral zone for

each compound, eliminating from the calculation the highest and the lowest values, due to the possible overlap of emission features over two contiguous zones.

Table 3. Average lifetime values (τ/ns) recorded from solid sample in the four spectral range (see text for details)

	α	β	γ	δ
τ_1	114.7	229.9	564.7	680.0
τ_2	27.5	42.1	136.6	138.4
τ_3	6.1	10.2	34.9	36.3

As evidenced, there is a growth of the lifetime values on moving toward the lower energy bands *i.e.* α towards δ), and this behavior can be due to the presence of 'aggregation-induced phosphorescent emission' (AIPE), which was claimed to be related to the presence of an intermolecular excimer formation in the solid state [23]: indeed, such excimer could cause a lifetime lengthening and a red-shifted emission, so the three-exponential decay of each compound can be attributed to the simultaneous presence of single molecule with aggregate ones. Complexes **1**-**12** show a wide lifetime variation also for molecules with the same substituent and the same counterion (Table S2 in see SI), suggesting that the aggregation modes is related to stereoisomerism.

4. Conclusions

This paper represents a further step in the systematic research of stereoselective synthesis of coordination compounds. In this work we have successfully synthesized, separated and characterized three series of new octahedral ionic Ir(III) complexes with a dual stereogenic center, at-metal and at-ligand. By using camphorsulfonate as resolving anion, we have separated diasterosomeric couples thus obtaining twelve enantiomerically pure complexes. The absolute metal configuration was assigned based on specific pattern of NOE cross-peak, DFT calculations and confirmed by ECD spectra. ^{1}H-NMR experiments also showed a strong interaction of the complexes with the counteranion that caused a remarkable high frequencies shift of the involved protons. Several investigations have been carried out on chiral Ir(III) complexes, in order to enlight

if any the correlation between stereoisomerism and photophysical properties. Valuable results have been obtained by exploring polarized emission, but efforts have been directed towards the search of a link between symmetry related to isomerism and photophysics. We have performed a wide and accurate investigation on three homologous series of complexes and results shed light on a possible link between electronic spectroscopy and stereoisomerism: indeed, despite the different stereochemistry, all the investigated compounds display similar photophysical properties in solution. Differences were found by exploring photophysics in solid state. Although the complexity of the emission spectra it has been possible to reduce the luminescence to common factors to the twelve complexes, which reflect the influence of the stereochemistry. Thus, such influence could reasonably awaited to a different packing of the enantiomers and diastereoisomers that produces aggregates with different emitting properties, attributable to the presence of AIPE.

Appendix A. Supporting information

Supplementary data associated with this article can be found in the online version at……

References

[1] M.K. Nazeeruddin, C. Klein, M. Grätzel, L. Zuppiroli, D. Berner, Molecular engineering of iridium complexes and their application in organic light emitting devices, in: Y. H. Weinheim (Eds.), Highly

efficient OLEDs with phosphorescent materials, Wiley-VCH, Germany, 2008, pp. 363-387; Z. Chen, Z. Bian, C. Huang, Functional Ir[III] complexes and their applications, Adv. Mater. 22 (2010) 1534-1539; Y. You, W. Nam, Photofunctional triplet excited states of cyclometalated Ir(III) complexes: beyond electroluminescence, Chem. Soc. Rev. 41 (2012) 7061-7084; C. Ulbricht, B. Beyer, C. Friebe, A. Winter, U.S. Schubert, Recent developments in the application of phosphorescent Iridium(III) complex systems, Adv. Mater. 21 (2009) 4418-4441; H. Yersin, A.F. Rausch, R. Czerwieniec, T. Hofbeck, T. Fischer, The triplet state of organo-transition metal compounds. Triplet harvesting and singlet harvesting for efficient OLEDs, Chem. Soc. Rev. 255 (2011) 2622-2652.

[2]   Y. You, Phosphorescence bioimaging using cyclometalated Ir(III) complexes, Curr. Opin. Chem. Biol. 17 (2013) 699-707; T. Yoshihara, M. Hosaka, M. Terata, K. Ichikawa, S. Murayama, A. Tanaka, M. Mori, H. Itabashi, T. Takeuchi, S. Tobita, Intracellular and in vivo oxygen sensing using phosphorescent Ir(III) complexes with a modified acetylacetonato ligand, Anal. Chem. 5 (2015) 2710-2717; Q. Zhao, C. Huang, F. Li, Phosphorescent heavy-metal complexes for bioimaging, Chem. Soc. Rev. 40 (2011) 2508-2524; K.K-W. Lo K.Y. Zhang, Iridium(III) complexes as therapeutic and bioimaging reagents for cellular applications, RSC Adv. 2 (2012) 12069-12083; K.K.-W. Lo, M-W. Louie, K.Y. Zhang, Design of luminescent iridium(III) and rhenium(I) polypyridine complexes as in vitro and in vivo ion, molecular and biological probes, Coord. Chem. Rev. 254 (2010) 2603-2622; P. Sun, X. Lu, Q. Fan, Z. Zhang, W. Song, B. Li, L- Huang, J. Peng, W. Huang, Water-soluble iridium(III)-containing conjugated polyelectrolytes with weakened energy transfer properties for multicolor protein sensing applications, Macromolecules 44 (2011) 8763-8770; K.K. Lo, A.W. Choi, W.H. Law, Applications of luminescent inorganic and organometallic transition metal complexes as biomolecular and cellular probes, Dalton Trans. 41 (2012) 6021-6047; Y. Chen, L. Qiao, L-Ji, H. Chao, Phosphorescent iridium(III) complexes as multicolor probes for specific mitochondrial imaging and tracking, Biomaterials 35 (2014) 2-13.

[3]   L. Ricciardi, T.F. Mastropietro, M. Ghedini, M. La Deda, E.I. Szerb, Ionic-pair effect on the phosphorescence of ionic Iridium(III) complexes, J. Organomet. Chem. 772-773 (2014) 307-313.

[4]   Y.J. Yadav, B. Heinrich, G. De Luca, A.M. Talarico, T.F. Mastropietro, M. Ghedini, B. Donnio, E.I. Szerb, Chromonic-like physical luminescent gels formed by ionic octahedral iridium(III) complexes in diluted water solutions, Adv. Opt. Mater. 1 (2013) 844-854.

[5]   J. Ma, X. Ding, Y. Hu, Y. Huang, L. Gong, E. Meggers, Metal-templated chiral brønsted base organocatalysis, Nature Commun. 5 (2014) 5531; L. Gong, L.-A. Chen, E. Meggers, Asymmetric catalysis mediated by the ligand sphere of octahedral chiral-at-metal complexes, Angew. Chem. Int. Ed. 53 (2014) 10868-10874; E.B. Bauer, Chiral-at-metal complexes and their catalytic applications in organic synthesis, Chem. Soc. Rev. 41 (2012) 3153-3167; Recent advances in the use of chiral metal complexes with achiral ligands for application in asymmetric catalysis, Catal. Sci. Technol. (2015) DOI: 10.1039/C5CY00182J.

[6]   L. Feng, Y. Geisselbrecht, S. Blanck, A. Wilbuer, G.E. Atilla-Gokcumen, P. Filippakopoulos, K. Kräling, M. A. Celik, K. Harms, J. Maksimoska, R. Marmorstein, G. Frenking, S. Knapp, L.-O. Essen, E. Meggers, Structurally sophisticated octahedral metal complexes as highly selective protein kinase inhibitors, J. Am. Chem. Soc. 133 (2011) 5976-5986.

[7]   P. Göbel, F. Ritterbusch, M. Helms, M. Bischof, K. Harms, M. Jung, E. Meggers, Probing chiral recognition of enzyme active sites with octahedral iridium(III) propeller complexes, Eur. J. Inorg. Chem. (2015) 1654-1659. doi: 10.1002/ejic.201500087.

[8]   E.K. Martina, N. Paganoa, M.E. Sherlocka, K. Harmsa, E. Meggers, Synthesis and anticancer activity of ruthenium half-sandwich complexes comprising combined metal centrochirality and planar chirality, Inorg. Chim. Acta. 423 (2014) 530-539.

[9]   D. Zerla, G. Facchetti, M. Fusè, M. Pellizzoni, C. Castellano, E. Cesarotti, R. Gandolfi, I. Rimoldi, 8-Amino-5,6,7,8-tetrahydroquinolines as ligands in iridium(III) catalysts for the reduction of aryl ketones by asymmetric transfer hydrogenation (ATH), Tetrahedron: Asymmetry. 25 (2014) 1031-1037.

[10] I. Rimoldi, G. Facchetti, E. Cesarotti, M. Pellizzoni, M. Fusè, D. Zerla, Enantioselective transfer hydrogenation of aryl ketones: synthesis and 2D-NMR characterization of new 8-amino-5,6,7,8-tetrahydroquinoline Ru(II)-complexes, Curr. Org. Chem. 16 (2012) 2982-2988.

[11] M. Nonoyama, Benzo[h]quinolin-10-yl-N iridium(III) complexes, Bull. Chem. Soc. Jpn. 47 (1974) 767-768.

[12] S. Sprouse, K.A. King, P.J. Spellane, R.J. Watts, Photophysical effects of metal-carbon σ bonds in ortho-metalated complexes of Ir(III) and Rh(III), J. Am. Chem. Soc. 106 (1984) 6647-6653.

[13] T.F. Mastropietro, Y.J. Yadav, E.I. Szerb, A.M. Talarico, M. Ghedini, A. Crispini, Luminescence mechanochromism in cyclometallated Ir(III) complexes containing picolylamine, Dalton Trans. 41 (2012) 8899-8907.

[14] J. N. Demas, G. A. Crosby, Measurement of photoluminescence quantum yields. Review, J. Phys. Chem. 75 (1971) 991-1024.

[15] K. Nakamaru, Luminescence quantum yields, and lifetimes of trischelated ruthenium(II) mixed-ligand complexes including 3,3′-dimethyl-2,2′-bipyridyl, Bull. Soc. Chem. Jpn. 5 (1982) 2697-2705.

[16] P.J. Spellane, R.J. Watts, C.J. Curtis, Analysis of the proton and carbon-13 NMR spectra of [Ir(Hbpy-C3,N')(bpy-N,N')2]$^{3+}$: evidence for a carbon-bonded structure, Inorg. Chem. 22 (1983) 4060-4062.

[17] E. Marchi, R. Sinisi, G. Bergamini, M. Tragni, M. Monari, M. Bandini, P. Ceroni, Easy separation of Δ and Λ isomers of highly luminescent [IrIII]-cyclometalated complexes based on chiral phenol-oxazoline ancillary ligands, Chem. - A Eur. J. 18 (2012) 8765-8773.

[18] M. Helms, Z. Lin, L. Gong, K. Harms, E. Meggers, Method for the preparation of non-racemic bis-cyclometalated iridium(III) complexes, Eur. J. Inorg. Chem. 2013 (2013) 4164-4172.

[19] A.B. Tamayo, S. Garon, T. Sajoto, P.I. Djurovich, I.M. Tsyba, R. Bau, M.E. Thompson, Cationic bis-cyclometalated iridium(III) diimine complexes and their use in efficient blue, green, and red electroluminescent devices, Inorg. Chem. 44 (2005) 8723-8732; S. Lamansky, P. Djurovich, D. Murphy, F. Abdel-Razzaq, H-E. Lee, C. Adachi, P.E. Burrows, S.R. Forrest, M. E. Thompson, Highly phosphorescent bis-cyclometalated iridium complexes: synthesis, photophysical characterization, and use in organic light emitting diodes, J. Am. Chem. Soc. 123 (2001) 4304-4312.

[20] A. Auffrant, A. Barbieri, F. Barigelletti, J. Lacour, P. Mobian, J.P. Collin, J.P. Sauvage, B. Ventura, Iridium(III) complexes consisting of Ir(ppy)(2) units (ppy= 2-phenylpyridine) and two laterally connected N⋀N chelates as bridge: synthesis, separation, and photophysical properties, Inorg Chem. 46 (2007) 6911-6919; L. Flamigni, A. Barbieri, C. Sabatini, B. Ventura, F. Barigelletti, Photochemistry and photophysics of coordination compounds: Iridium, Top. Curr. Chem. 281 (2007) 143-203.

[21] R.D. Costa, E. Ortì, H.J. Bolink, F. Monti, G. Accorsi, N. Armaroli, Luminescent ionic transition-metal complexes for light-emitting electrochemical cells, Angew. Chem. Int. Ed. 51 (2012) 8178-8211.

[22] C. Schaffner-Hamann, A. von Zelewsky, A. Barbieri, F. Barigelletti, G. Muller, J.P. Riehl, A. Neels, Diastereoselective formation of chiral tris-cyclometalated iridium(III) complexes: characterization and

photophysical properties, J. Am. Chem. Soc. 126 (2004) 9339-9348.

[23] Q. Zhao, L. Li, F. Li, M. Yu, Z. Liu, T. Yi, C. Huang, Aggregation-induced phosphorescence emission (AIPE) of iridium (III) complexes, Chem. Commun. 685 (2008) 685-687; G.G.Shan, L.Y. Zhang, H.B. Li, S. Wang, D.X. Zhu, P. Li, C.G. Wang, Z.M. Su, Y. Liao, A cationic iridium(III) complex showing aggregation-induced phosphorescent emission (AIPE) in the solid state: synthesis, characterization and properties, Dalton Trans. 41 (2012) 523-530.